Synthesis and Magnetic Properties of Iron(III) Complexes bridged by 1,1′-Tetramethylenediimidazole exhibiting an Infinite Zigzag-chain Structure†

Mika Fukuya, Masaaki Ohba, Ken-ichiro Motoda, Naohide Matsumoto,* Hisashi Ōkawa and Yonezo Maeda

Department of Chemistry, Faculty of Science, Kyushu University, Hakozaki, Higashi-ku, Fukuoka 812, Japan

Three polymeric iron(III) complexes $[Fe(tdim)L^n]ClO_4$ ($L = L^1$ **1**, L^2 **2** or L^3 **3**) consisting of a bridging ligand (tdim = 1,1′-tetramethylenediimidazole) and a quadridentate Schiff base ligand have been prepared and characterized, where $H_2L^n = RN(CH_2)_2NR'$ [R = R′ = MeC(OH)=CHCMe=, $n = 1$; R = R′ = o-HOC_6H_4CH=, $n = 3$; R = MeC(OH)=CHCMe=, R′ = o-HOC_6H_4CH=, $n = 2$]. Magnetic susceptibility data (4.2–300 K) showed that **1** is low spin ($S = \frac{1}{2}$), **2** of spin equilibrium ($S = \frac{5}{2} \rightleftharpoons \frac{1}{2}$), and **3** essentially high spin ($S = \frac{5}{2}$) and exhibiting an unusual behaviour below *ca.* 100 K. The spin equilibrium of **2** occurs over a wider temperature range than that of the corresponding mononuclear complex $[Fe(mim)_2L^2]ClO_4$ (mim = 1-methylimidazole). A crystal structure analysis of **3** confirmed that it has an infinite zigzag-chain structure and the iron(III) ion is six-co-ordinated by N_2O_2 donor atoms of the quadridentate ligand, an imidazole nitrogen atom of a bridging ligand and a nitrogen atom of the adjacent bridging ligand. The crystal structure also shows that **3** suffers from disorder and there are two configurations **A** and **B** with respect to the orientation of the imidazole moiety, having populations of 0.65 and 0.35, respectively. The unusual magnetic behaviour is rationalized by the crystal structure, Mössbauer and ESR spectra.

According to the Tanabe–Sugano diagram for the d^5 electronic configuration in an O_h ligand field[1] three types of electronic structures are expected depending on the ligand-field strength, *i.e.* high spin ($S = \frac{5}{2}$), spin equilibrium ($S = \frac{5}{2} \rightleftharpoons \frac{1}{2}$), and low spin ($S = \frac{1}{2}$). In fact all three types of six-co-ordinate iron(III) complexes are known.[2] Among them, those exhibiting spin-equilibrium behaviour have attracted much attention. A number of six-co-ordinate iron(III) complexes with Schiff-base ligands exhibiting such behaviour have been prepared and it is found that the spin state is determined primarily by the ligand-field strength.[3,4] It has been also pointed out that the mechanism of spin-equilibrium behaviour cannot be explained only in terms of an iron(III) complex molecule as an isolated system.[5] We are interested in bi- and poly-nuclear iron(III) complexes exhibiting spin-equilibrium behaviour.[6] In this study, in order to determine the influence of polymeric structure on spin-equilibrium behaviour, three polymeric iron(III) complexes $[Fe(tdim)L^n]ClO_4$ ($L = L^1$ **1**, L^2 **2** or L^3 **3**) consisting of a bridging ligand (tdim = 1,1′-tetramethylenediimidazole) and a quadridentate Schiff-base ligand (H_2L^n, n = 1–3) have been prepared, where the schematic structures of the ligands are as shown. The equatorial ligands of **1**, **2** and **3** are selected so as to give low-spin, spin-equilibrium, and high-spin complexes, respectively.

Experimental

CAUTION: Perchlorate salts are potentially explosive and should only be handled in small quantities.

Syntheses.—Ligands. The compound tdim was prepared according to the literature.[7] The symmetrical quadridentate ligands H_2L^1 and H_2L^3 were prepared by mixing salicylaldehyde or acetylacetone and ethylenediamine in 2:1 molar ratio in methanol. The unsymmetrical ligand H_2L^2 was prepared as follows. The copper(II) complex $[CuL^2]$ was prepared according to the method of Kuska *et al.*[8] and the demetallation reaction by H_2S gas in dichloromethane gave the ligand H_2L^2 as yellow oily material.

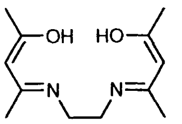

H_2L^1

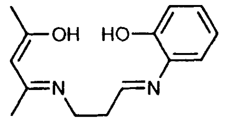

H_2L^2

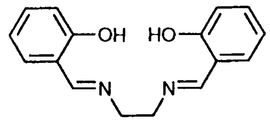

H_2L^3

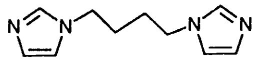

tdim

$[Fe(mim)_2L^n]ClO_4$ (mim = *1-methylimidazole*, n = 1–3). These mononuclear complexes were prepared as references according to the literature method.[3,4]

$[Fe(tdim)L^n]ClO_4$ **1**–**3**. These complexes were prepared in a similar way and the synthesis of **1** is described in detail as an example. To a solution of $[FeCl(L^1)]$[6] (166 mg, 0.5 mmol) in methanol (40 cm^3) was added a solution of tdim (95 mg, 0.5 mmol) in methanol (10 cm^3). The solution was warmed on a hot plate and filtered. To the filtrate was added a solution of sodium perchlorate (60 mg, 0.5 mmol) in methanol (10 cm^3). The solution was allowed to stand for several hours, during which time blue-green crystals precipitated. They were filtered off and washed with small amounts of methanol and diethyl ether, yield 210 mg (74%), m.p. 191–198 °C. IR: 3450(br), 3150, 2950, 1580, 1500, 1400 and 1100 cm^{-1} (Found: C, 45.25; H, 5.85;

---

† *Supplementary data available* (No. SUP 56968, 7 pp): magnetic susceptibilities and ESR spectra. See Instructions for Authors, *J. Chem. Soc., Dalton Trans.*, 1993, Issue 1, pp. xxiii–xxviii.

Non-SI units employed: G = 10^{-4} T, emu = $10^6/4\pi$SI, $\mu_B = 9.274 \times 10^{-24}$ J T^{-1}.

Fe, 9.45; N, 14.20. Calc. for $C_{22}H_{32}ClFeN_6O_6\cdot H_2O$: C, 45.10; H, 5.85; Fe, 9.55; N, 14.35%).

Complex **2**: red-brown crystals, yield 130 mg (44%), m.p. 173–180 °C. IR: 3400(br), 3100, 2950, 1620, 1440, 1100 and 620 cm^{-1} (Found: C, 48.30; H, 5.00; Fe, 9.15; N, 13.85. Calc. for $C_{24}H_{30}ClFeN_6O_6\cdot 0.5H_2O$: C, 48.15; H, 5.20; Fe, 9.35; N, 14.05; Fe, 9.35%).

Complex **3**: red-brown crystals, yield 130 mg, 44%, m.p. 241–247 °C. IR: 3400(br), 3100, 2950, 1620, 1440, 1100 and 620 cm^{-1} (Found: C, 50.80; H, 4.60; Fe, 9.10; N, 13.50. Calc. for $C_{26}H_{28}ClFeN_6O_6$: C, 51.05; H, 4.60; Fe, 9.15; N, 13.75%).

Physical Measurements.—Elemental analyses (C, H and N) were performed at the Elemental Analysis Service Center of Kyushu University. Iron analyses were made on a Shimadzu AA-680 atomic absorption/flame emission spectrophotometer. Infrared spectra were measured on KBr disks with a JASCO IR-810 spectrophotometer. Melting points were measured on a Yanagimoto apparatus and were uncorrected. Electrical conductivities were measured on a Denki Kagaku Keiki AOL-10 digital conductometer in *ca.* 10^{-3} mol dm^{-3} acetonitrile solutions. Electronic spectra were measured on a Shimadzu MPS-2000 multipurpose recording spectrophotometer, ESR spectra (X-band) of polycrystalline samples on a JES-FE3X spectrometer at liquid-nitrogen and room temperature. Magnetic susceptibilities were obtained at 4.2–100 K by use of a HOXAN HSM-2000 SQUID magnetometer and at 80–300 K by a Faraday balance designed in our laboratory. The calibration was made with $Mn(NH_4)_2(SO_4)_2\cdot 6H_2O$ for the SQUID susceptometer and with $[Ni(en)_3][S_2O_3]$ (en = ethylenediamine) for the Faraday balance.[9] Data were corrected for magnetization of the sample holder and for the diamagnetism of the component atoms by the use of Pascal constants.[10] The molar effective magnetic moments were calculated by the equation $\mu_{eff} = 2.828(\chi_M T)^{\frac{1}{2}}$. Mössbauer spectra were measured by using equipment previously described,[11] and fitted to Lorentzian line shapes by using a least-squares method at the Computer Center, Kyushu University. Isomer shifts are reported with respect to the centroid of the spectrum of iron foil enriched with ^{57}Fe at 296 K.

X-Ray Crystallography.—Crystals of complex **3** suitable for X-ray diffraction study were obtained by slow evaporation of a dichloromethane–methanol solution of the complex. A large crystal was cut to give a crystal with dimensions 0.4 × 0.4 × 0.3 mm. Reflection data were measured on a Rigaku Denki AFC-5 automated four-circle diffractometer with graphite-monochromatized Mo-Kα radiation at room temperature. Three standard reflections were monitored every 100 and showed no systematic decrease in intensity. The data were corrected for Lorentz and polarization factors, but not for absorption owing to the shape of the crystal. Unit-cell parameters were determined from 25 reflections in the range $20 < 2\theta < 30°$.

Crystal data for $[Fe(tdim)L^3]ClO_4$ **3**. $C_{26}H_{28}ClFeN_6O_6$, $M = 611.85$, monoclinic, space group $P2_1/a$, $a = 16.860(2)$, $b = 15.908(2)$, $c = 10.580(1)$ Å, $\beta = 103.950(8)°$, $U = 2754.0(5)$ Å^3, $F(000) = 1268$, μ(Mo-Kα) = 6.933 cm^{-1}, $D_c = 1.476$ g cm^{-3} ($Z = 4$), $D_m = 1.470$ g cm^{-3} (by flotation in aqueous KI solution), scan mode θ–2θ, scan speed 4° min^{-1}, scan range $2.5 < 2\theta < 50°$, scan width $(1.4 + 0.35 \tan\theta)°$, quadrant measured $+h$, $+k$, $\pm l$, reflections measured 4267, observed reflections with $|F_o| > 3\sigma(|F_o|)$ 3783, $R = 0.049$, $R' = 0.048$, weighting scheme $w = 1/\sigma^2(F_o)$, largest residue in the final Fourier difference synthesis 0.7 e Å^{-3}.

The structure was solved by the direct method (MULTAN 78)[12] and determined by Fourier and difference Fourier syntheses. The asymmetric unit consists of $[Fe(tdim)L^3]ClO_4$. In the course of the structure determination it was found that one of two imidazole moieties [N(5), C(23), C(24), C(25)] is subject to disorder. A difference Fourier map showed that there are two configurations **A** and **B** (see Fig. 4), the occupancy factors of which were initially assigned on the basis of the peak height and finally determined to be 0.65 and 0.35 by least-squares calculation. Refinement was carried out by the full-matrix least-squares method, the function minimized being $\Sigma w(|F_o| - |F_c|)^2$ and the weighting scheme $1/\sigma^2(F_o)$ for all reflections. The hydrogen atoms bound to carbon were introduced in calculated positions. They were included in the structure-factor calculation but not refined. Atomic scattering factors were taken from ref. 13. All computations were performed on a FACOM M 780 computer at the Computer Center of Kyushu University using the UNICS III program system.[14] The final atomic parameters are given in Table 1.

Additional material available from the Cambridge Crystallographic Data Centre comprises H-atom coordinates, thermal parameters and remaining bond lengths and angles.

Results and Discussion

The temperature dependences of the effective magnetic moments for complexes **1–3** and the reference $[Fe(mim)_2L^2]ClO_4$ are shown in Fig. 1. The polycrystalline ESR spectra of **1–3** and of the corresponding mononuclear complexes $[Fe(mim)_2L^n]ClO_4$ (n = 1–3) were measured at 80 K and are available as SUP 56968. The Mössbauer spectra were measured at 296 and 78 K, and the data are summarized in Table 2.

$[Fe(tdim)L^1]ClO_4$ **1**. The effective magnetic moment is 2.48 μ_B at 290 K and 2.13 μ_B at 82 K, indicating that complex **1** is essentially low spin ($S = \frac{1}{2}$) in the temperature range measured. The ESR spectrum at liquid-nitrogen temperature showed three sharp signals at $g_1 = 2.294$, $g_2 = 2.147$ and $g_3 = 1.971$ and resembles that of the low-spin mononuclear complex $[Fe(mim)_2L^1]ClO_4$ ($g_1 = 2.344$, $g_2 = 2.129$, $g_3 = 1.952$). The reflectance spectra of **1** and $[Fe(mim)_2L^1]ClO_4$ both showed a broad absorption at *ca.* 670 nm which is characteristic of low-spin iron(III) species with this ligand system,[3,4] while the starting chloro complex $[FeCl(L^1)]$ showed a broad band at 510 mm. The Mössbauer spectra showed a doublet with quadruple splitting $\Delta E = 2.15$ mm s^{-1} and isomer shift $\delta = 0.19$ mm s^{-1} at 78 K and $\Delta E = 2.13$ mm s^{-1} and $\delta = 0.14$ mm s^{-1} at 296 K. These parameters are characteristic of low-spin iron(III) species.[15]

$[Fe(tdim)L^2]ClO_4$ **2**. The effective magnetic moment is 5.37 μ_B at 290 K slightly smaller than the spin-only value 5.92 μ_B of high-spin Fe^{III} ($S = \frac{5}{2}$). As the temperature is lowered the magnetic moment decreases linearly from 5.37 μ_B at 290 K to 3.37 μ_B at 4.2 K, accompanied by a change from red-brown to blue-green. This behaviour is attributable to a spin equilibrium

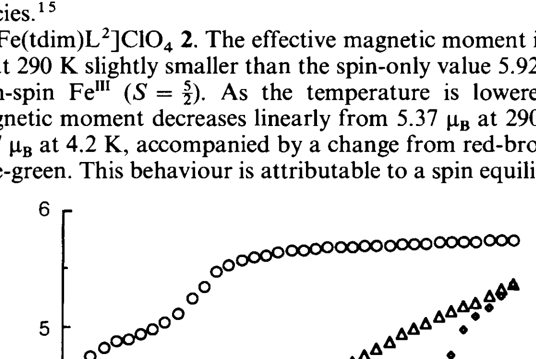

Fig. 1 Temperature dependence of the effective magnetic moment μ_{eff} per iron for polycrystalline samples of complexes **1** (□), **2** (△), **3** (○) and $[Fe(mim)_2L^2]ClO_4$ (◇)

Table 1 Atomic coordinates (× 10^4) for [Fe(tdim)L^3]ClO_4 **3**

Atom	*x*	*y*	*z*	Atom	*x*	*y*	*z*
Fe	488.3(4)	1698.6(4)	1894.6(6)	C(13)	2950(4)	1967(3)	−808(5)
O(1)	−577(2)	1243(2)	1551(3)	C(14)	2259(4)	1669(3)	−1661(4)
O(2)	748(2)	1758(2)	244(3)	C(15)	1527(4)	1603(3)	−1303(4)
N(1)	496(2)	1703(2)	3907(3)	C(16)	1461(4)	1823(2)	−42(4)
N(2)	1627(2)	2261(2)	2742(3)	C(17)	675(3)	−261(3)	1668(4)
N(3)	1050(3)	473(2)	2189(3)	C(18)	1223(4)	−894(3)	1887(5)
N(4)	1949(3)	−560(2)	2567(4)	C(19)	1816(3)	264(3)	2719(4)
N(5)	4717(6)	734(5)	2306(7)	C(20)	2738(4)	−1003(3)	3041(5)
N(5*)	4477(12)	843(10)	1661(15)	C(21)	3208(4)	−1097(3)	2007(6)
N(6)	5074(3)	2015(2)	1714(4)	C(22)	3550(4)	−272(3)	1599(6)
C(1)	−1054(3)	990(3)	2298(5)	C(23)	4236(4)	88(4)	2664(7)
C(2)	−1817(4)	635(3)	1699(5)	C(24)	5187(7)	617(5)	1455(9)
C(3)	−2349(4)	361(3)	2442(6)	C(24*)	4619(10)	899(9)	450(14)
C(4)	−2132(4)	421(4)	3774(6)	C(25)	5425(6)	1382(5)	1136(8)
C(5)	−1395(4)	772(4)	4379(5)	C(25*)	4947(11)	1659(9)	369(15)
C(6)	−838(3)	1064(3)	3678(4)	C(26)	4702(3)	1566(3)	2447(5)
C(7)	−73(4)	1416(3)	4391(4)	Cl	−1080(1)	3407(1)	5862(1)
C(8)	1269(3)	1983(3)	4769(4)	O(3)	−285(3)	3311(3)	5677(5)
C(9)	1692(3)	2591(3)	4058(4)	O(4)	−1391(4)	2662(3)	6294(5)
C(10)	2202(3)	2375(3)	2163(4)	O(5)	−1585(4)	3639(4)	4664(6)
C(11)	2180(3)	2123(2)	841(4)	O(6)	−1071(4)	4037(4)	6759(7)
C(12)	2907(4)	2202(3)	430(5)				

Occupancy factor 0.65 for N(5), C(24) and C(25); occupancy factor 0.35 for N(5*), C(24*) and C(25*).

Table 2 Mössbauer spectral data (mm s^{-1}) for complexes **1**–**3**

	78 K			296 K	
Complex	Δ*E*	δ	*A*[a] (%)	Δ*E*	δ
1	2.15	0.19		2.13	0.14
2	2.37	0.20	74	*b*	
	1.29	0.48	26		
3	2.26	0.24	29	*b*	
	1.24	0.53	71		

[a] Population (the fraction of absorption area). [b] Not observed.

between high- and low-spin states of Fe^{III}. It was also confirmed that the spin-equilibrium behaviour of **2** does not present a thermal hysteresis. The spin equilibrium occurs over a wider temperature range than that of the corresponding mononuclear complex [Fe(mim)$_2L^2$]ClO_4 as shown in Fig. 1. The ESR spectrum at 78 K showed two broad absorptions around 1500 and 3000 G, the former being characteristic of high-spin species and the latter of low-spin iron(III) species. On the other hand, the spectrum of the reference mononuclear complex at 78 K showed only a broad signal around 3000 G. The ESR spectral data are consistent with the magnetic susceptibility data in that the conversion from the high- to the low-spin state is completed in [Fe(mim)$_2L^2$]ClO_4 at 78 K but not completed at this temperature in **2**. The Mössbauer spectrum of **2** was not observed at 296 K because of the low recoilless fraction of the complex. However, at 78 K a spectrum with two doublets assignable to high- (ΔE = 1.29 and δ = 0.48 mm s^{-1}) and low-spin (ΔE = 2.37 and δ = 0.20 mm s^{-1}) species was observed. The population of low-spin isomer is calculated to be 74% at 78 K from the area of the Mössbauer absorption under the assumption that the recoilless fraction of the high-spin species is equivalent to that of the low-spin one.

[Fe(tdim)L^3]ClO_4 **3**. The effective magnetic moment is 5.76 μ_B at 290 K, close to the spin-only value 5.92 μ_B for $S = \frac{5}{2}$. As the temperature is lowered μ_{eff} is practically constant in the range *ca.* 290–100 K, then decreases from 5.48 μ_B at 98 K reaching a plateau of 4.90 μ_B at 42 K, and finally decreases abruptly to 4.42 μ_B at 4.2 K. This behaviour is unusual, because the μ_{eff} *vs.* *T* curve shows two magnetic processes (first at 300–40 K, second at < 40 K) and the lowest μ_{eff} value is too high for a simple spin-equilibrium behaviour. The polycrystalline ESR spectrum of **3** at 78 K shows two sets of absorptions around 1400 and 2500–3500 G. The former broad absorption is attributable to a high-spin species, because the ESR spectrum of the high-spin mononuclear reference complex [Fe(mim)$_2L^3$]ClO_4 showed a similar broad signal around 1500 G and is well known to be typical of high-spin iron(III) complexes.[3] The latter absorption is attributable to a low-spin species, because three signals are typical of low-spin species such as **1** and the related low-spin mononuclear iron(III) complexes.[3,4] The ESR spectrum indicated that **3** contains both high- and low-spin iron(III) species at 78 K. The Mössbauer spectrum was not observed at 296 K because of the low recoilless fraction of the complex. However, at 78 K a spectrum with two doublets was observed, where that with ΔE = 1.24 and δ = 0.53 mm s^{-1} is attributable to a high-spin species and the other with ΔE = 2.26 and δ = 0.24 mm s^{-1} is due to a low-spin species. The population of the low-spin isomer is calculated to be 29% at 78 K from the area of the Mössbauer absorption.

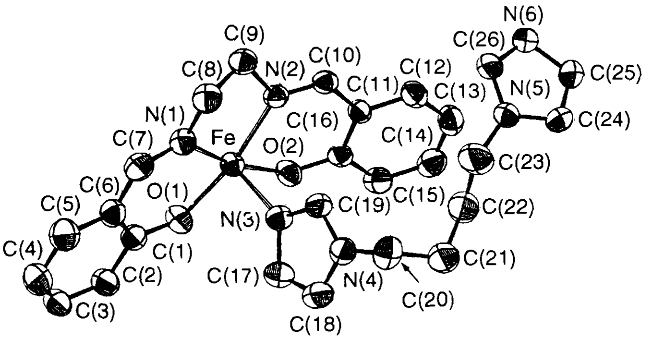

Fig. 2 An ORTEP drawing of the cation of [Fe(tdim)L^3]ClO_4 **3** with the atom numbering scheme, where the thermal ellipsoids are drawn at 50% probability level

Crystal Structure of Complex **3**.—An ORTEP[16] drawing of complex **3** with the atom numbering scheme is shown in Fig. 2. The crystal structure projected on the *ab* plane is given in Fig. 3, and selected bond distances and angles with their estimated standard deviations are in Table 3. The crystal of complex **3** is isomorphous to the corresponding manganese(III) complex the crystal structure of which was reported previously.[17] It has an infinite zigzag-chain structure bridged by two imidazole

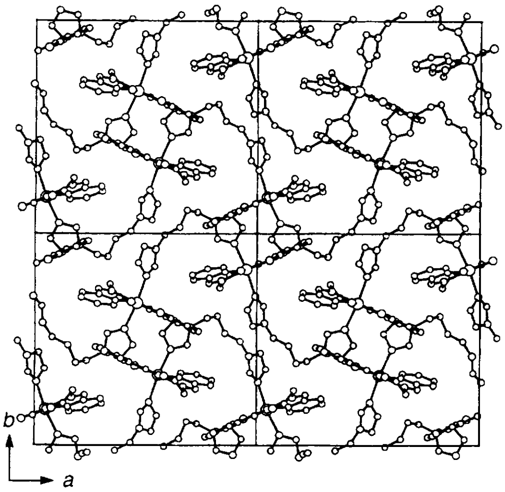

Fig. 3 Molecular packing of [Fe(tdim)L^3]ClO_4 **3** in the crystal, showing the zigzag chain structure

Table 3 Selected bond distances (Å) and angles (°)

Fe–O(1)	1.889(3)	Fe–O(2)	1.902(3)
Fe–N(1)	2.126(4)	Fe–N(2)	2.113(4)
Fe–N(3)	2.157(4)	Fe–N(6′)	2.156(4)
O(1)–N(1)	1.318(7)	O(2)–C(16)	1.313(7)
N(1)–C(7)	1.276(8)	N(1)–C(8)	1.468(6)
N(2)–C(9)	1.467(6)	N(2)–C(10)	1.278(7)
C(1)–C(2)	1.408(7)	C(1)–C(6)	1.421(7)
C(2)–C(3)	1.397(9)	C(3)–C(4)	1.371(9)
C(4)–C(5)	1.373(9)	C(5)–C(6)	1.407(9)
C(6)–C(7)	1.442(7)	C(8)–C(9)	1.506(8)
C(10)–C(11)	1.447(6)	C(11)–C(12)	1.403(9)
C(11)–C(16)	1.422(7)	C(12)–C(13)	1.381(8)
C(13)–C(14)	1.375(8)	C(14)–C(15)	1.379(9)
C(15)–C(16)	1.410(7)		
O(1)–Fe–O(2)	105.2(1)	O(1)–Fe–N(1)	88.3(1)
O(1)–Fe–N(2)	165.7(1)	O(1)–Fe–N(3)	92.6(2)
O(1)–Fe–N(6′)	94.3(2)	O(2)–Fe–N(1)	166.4(2)
O(2)–Fe–N(2)	89.0(2)	O(2)–Fe–N(3)	88.3(2)
O(2)–Fe–N(6′)	90.7(2)	N(1)–Fe–N(2)	77.8(2)
N(1)–Fe–N(3)	87.8(1)	N(1)–Fe–N(6′)	90.5(2)
N(2)–Fe–N(3)	89.9(1)	N(2)–Fe–N(6′)	88.0(2)
N(3)–Fe–N(6′)	172.9(2)		

Primed atoms at $x - \frac{1}{2}, -y + \frac{1}{2}, z$.

nitrogen atoms of tdim as depicted in Fig. 3. The iron(III) atom is six-co-ordinated by N_2O_2 donor atoms of the equatorial ligand L^3, an imidazole nitrogen atom of the tdim ligand N(3) and a nitrogen atom of the adjacent tdim ligand N(6′) ($x - \frac{1}{2}, -y + \frac{1}{2}, z$). The mean length of the co-ordination bonds, 2.057 Å, is similar to those of high-spin mononuclear complexes [Fe(Him)$_2L^3$]$ClO_4 \cdot H_2O$ (2.059 Å) (Him = imidazole) and [Fe(Him)$_2$(salphen)]BPh_4 (2.062 Å) [salphen = *N*,*N*′-bis-(salicyclidene)-*o*-phenylenediamine].[3,4]

It was found that there are two configurations with respect to the orientation of imidazole moiety (Fig. 4) where the population factors of **A** and **B** are estimated to be 0.65 and 0.35, respectively. The imidazole ring without disorder lies approximately on O(1)–Fe–N(2), while the other imidazole ring in configuration **A** lies on O(2)–Fe–N(1) and in **B** bisects O(1)–Fe–N(1).

At this stage it is appropriate to consider the unusual magnetic behaviour of complex **3**. Since the shortest Fe ··· Fe distance is 8.807(1) Å, **3** can be considered as a magnetically non-coupled system. Therefore, the decrease in the magnetic moment is not attributed to magnetic interaction but to spin equilibrium of iron(III) species. The magnetic moment in the plateau region, 4.90 μ_B, agrees well with the calculated value of 4.93 μ_B based on the assumption that the complex includes high- and low-spin iron(III) species with a mole ratio of 2 : 1 at 42 K. If the iron(III) species with configuration **A** remains in the high-spin state and that with **B** displays a conversion from high to low spin the temperature dependence of the effective magnetic moment can be rationalized. This is in accord with the ESR and Mössbauer spectral data. That the population of the low-spin isomer is 29% at 78 K from the area of the Mössbauer absorption is also nearly consistent with the X-ray and magnetic susceptibility results. Geiger *et al.*[18] pointed out that the relative orientation of the imidazole rings controls the spin state of porphyrin complexes. On the other hand, Nishida *et al.*[19] investigated a series of iron(III) complexes [FeB_2L] (**B** = pyridine and imidazole derivatives, L = quadridentate Schiff-base ligand such as L^1, L^2) and showed that there is no distinct correlation between the spin state and the orientation of the axial ligands. The present result indicates that the orientation of the axial ligands may be one of the determining factors of the spin state.

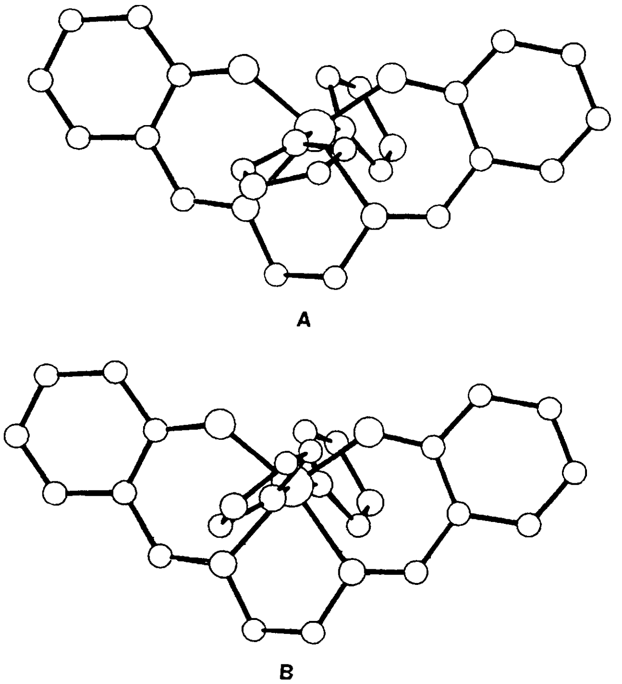

A

B

Fig. 4 The two configurations **A** and **B**, having occupancy factors of 0.65 and 0.35, respectively

Acknowledgements

This work was supported in part by a Grant-in-Aid for Scientific Research from the Ministry of Education, Science, and Culture (No. 04453048).

References

1 Y. Tanabe and S. Sugano, *J. Phys. Soc. Jpn.*, 1954, **9**, 753.
2 E. Sinn, G. Sim, E. V. Dose, M. F. Tweedle and L. J. Wilson, *J. Am. Chem. Soc.*, 1978, **100**, 3375; M. F. Tweedle and L. J. Wilson, *J. Am. Chem. Soc.*, 1976, **98**, 4824; T. Ito, M. Sugimoto, H. Ito, K. Toriumi, H. Nakayama, W. Mori and M. Sekizaki, *Chem. Lett.*, 1983, 121.
3 Y. Nishida, S. Oshio and S. Kida, *Chem. Lett.*, 1975, 59; *Bull. Chem. Soc. Jpn.*, 1977, **50**, 119; *Inorg. Chim. Acta*, 1977, **23**, 59; Y. Nishida, A. Sumita, H. Hayashida, H. Oshima, S. Kida and Y. Maeda, *J. Coord. Chem.*, 1979, **9**, 161.
4 Y. Maeda, Y. Takashima, N. Matsumoto and A. Ohyoshi, *J. Chem. Soc., Dalton Trans.*, 1986, 1115; N. Matsumoto, S. Ohta, C. Yoshimura, A. Ohyoshi, S. Kohata, H. Ōkawa and Y. Maeda, *J. Chem. Soc., Dalton Trans.*, 1985, 2575; N. Matsumoto, K. Kimoto, A. Ohyoshi and Y. Maeda, *Bull. Chem. Soc. Jpn.*, 1984, **57**, 3307.

5 E. König, G. Ritter, J. Dengler and S. M. Nelson, *Inorg. Chem.*, 1987, **26**, 3582.

6 S. Ohta, C. Yoshimura, N. Matsumoto, H. Ōkawa and A. Ohyoshi, *Bull. Chem. Soc. Jpn.*, 1986, **59**, 155.

7 W. Schtze and H. Schubert, *J. Prackt. Chem.*, 1959, **8**, 306.

8 H. A. Kuska, M. F. Farona, P. Pappas and S. Potterton, *J. Coord. Chem.*, 1971, **1**, 259; N. Matsumoto, M. Asakawa, H. Nogami and A. Ohyoshi, *Inorg. Chim. Acta*, 1985, **96**, 87.

9 L. F. Lindoy, V. Katovic and D. H. Busch, *J. Chem. Educ.*, 1972, **49**, 117.

10 E. A. Boudreaux and L. N. Mulay, in *Theory and Applications of Molecular Paramagnetism*, Wiley, New York, 1976, pp. 491–495.

11 Y. Maeda, M. Aramaki, Y. Takashima, Oogai and T. Goto, *Bull. Chem. Soc. Jpn.*, 1987, **60**, 3241.

12 P. Main, L. Lessinger, M. M. Woolfson, G. Germain and J. P. Declercq, MULTAN 78, A system of Computer Programs for The Automatic Solution of Crystal Structures from X-Ray Diffraction Data, Universities of York and Louvain, 1978.

13 *International Tables for X-Ray Crystallography*, Kynoch Press, Birmingham, 1974 vol. 4; R. F. Stewart, E. R. Davison and W. T. Simpson, *J. Chem. Phys.*, 1965, **42**, 3175.

14 T. Sakurai and K. Kobayashi, *Rikagaku Kenkyusho Houkoku*, 1979, **55**, 69; S. Kawano, *Rep. Comput. Kyushu Univ.*, 1980, **13**, 39.

15 N. N. Greenwood and T. C. Gibb, *Mössbauer Spectroscopy*, Chapman and Hall, London, 1971.

16 C. K. Johnson, ORTEP, Report ORNL-5138, Oak Ridge National Laboratory, Oak Ridge, TN, 1976.

17 N. Matsumoto, N. Takemoto, A. Ohyosi and H. Ōkawa, *Bull. Chem. Soc. Jpn.*, 1988, **61**, 2984.

18 D. K. Geiger, Y. J. Lee and W. R. Scheidt, *J. Am. Chem. Soc.*, 1984, **106**, 6339.

19 Y. Nishida, K. Kino and S. Kida, *J. Chem. Soc., Dalton Trans.*, 1987, 1157.

Received 11*th May* 1993; *Paper* 3/02668J